

## Dynamics Characteristics Analysis on Shaft Sprocket Assembly of Rake Conveyor

Eka Marliana\* and Ismail Ismail

*Department of Mechanical Engineering, Universitas 17 Agustus 1945 Surabaya, Indonesia*

(\*Corresponding author's e-mail: [ekamarliana@untag-sby.ac.id](mailto:ekamarliana@untag-sby.ac.id))

*Received: 28 January 2021, Revised: 20 June 2021, Accepted: 23 June 2021*

### Abstract

Every year, the Ngadirejo sugar factory encounters the same issue: The sprocket shaft of the eastern C2 rake conveyor at the boiler station fails. This conveyor is used to transfer bagasse from the mill to the kettle. As a result, when one of these components fails, the manufacturing process will be delayed. Static analysis was performed on a failing shaft in prior research, but the life cycle of the shaft was still relatively long. In this research, by employing HQ705 shaft materials, the modal and random vibration on the sprocket shaft was analyzed to determine the cause of this failure further. The analysis was carried out by using Ansys to implement the finite element method. This model used 8523 nodes and 4118 elements in the mesh. For modal analysis, as the number of orders increased, so did the frequency. The fourth and fifth-order vibrations included torsional vibration, with the most complex form, among others, with frequencies of 3061.6 and 3283.1 Hz. Maximum equivalent stress and maximum shear stress occurred at the exact location for static and random vibration analysis. The analysis is relevant to the actual failure that happened in reality.

**Keywords:** Failure, Modal, Shaft, Sprocket, Vibration

### Introduction

Every year, the Ngadirejo sugar plant always experiences failure on the shaft sprocket of the eastern C2 rake conveyor at the boiler station. This conveyor serves to distribute the bagasse to the kettle. So, when a failure occurs in these components, it will cause delays in the production process. The delay in the production process will cause financial losses for the company. In previous studies, static analysis has been carried out on the shaft that has failed, but the result is that the shaft life cycle is still quite long.

Many studies related to machine-based structures [1-3]. Rapid advancement in the finite element method is due to the advancement of powerful computer processors and software development. In recent years, the aid of finite elements in mechanical engineering has enormously increased [3,4]. The most critical factor in finite element analysis is numerical computations to estimate all parameters and boundaries agreed upon in the initial condition. It is a growing field that keeps evolving to meet the pace of growing science. Computer-aided design is used to analyze surfaces, search for optimum continuity, and assess the CMM data accuracy [5-7]. In order to broaden the knowledge and range of application, such as steam turbine engines, chatter turbine engines, plastic structures, apparatus, tools and furnitures, compressors, equipment, pumps, turbine blades, rotating shaft of the heating tanks, exhaust hoods rotors, turbine impellers, and support structures would solve the failure analysis for manufacturing equipment components. Fatigue is the gradual wear of material subjected to continual loads, generally separated into 3 stages; crack admittance, crack procreation, and unstable rapid growth [2,5-7].

The rake conveyor that is used here typically adopts chain and drive transmission. As a critical component, the chain and drive system are prone to encounter fatigue and vibration damage. The failure that occurs in this conveyor is not in the driveshaft but in the driven shaft. Specifically, it is located on the edge between the sprocket and the shaft. The failure in this shaft could be caused by fatigue or any other reason, such as vibration.

In many cases, vibration causes damage directly to the main mechanical component, such as the shaft, so that dynamic characteristics analysis needs to be conducted. In simulation or experiment analysis, one of the primary data that needs to be generated is the natural frequency. Furthermore, the critical speed of rotation is also meaningful. It is often close to the natural frequency. These characteristic

parameters and the results are needed to plot the resonance zone to monitor unit safety, including failure [8-12]. Therefore, this research will analyze the modal and random vibrations on the sprocket shaft to determine the cause of this failure further.

### Materials and methods

The shaft sprocket analyzed in this work is a component of the eastern C2 rake conveyor at the boiler station in the Ngadirejo sugar plant. This component's diameter is 150 mm, the length is 2000 mm, and the material is HQ705, which is equivalent to AISI 4340. The ultimate strength of this material is 900 MPa, the yield strength is 700 MPa, and the Poisson's ratio is 0.2 %.

The model for the shaft sprocket system in the rake conveyor unit comprises several parts: Shaft, sprocket, and the related bearing. To analyze the dynamic characteristics of the shaft, a simplified model will be used. The finite element method (FEM), which has high numerical stability, will be employed in order to analyze the shaft. This method is widely used to solve dynamic problems. The finite element method (FEM) key aims to transform the infinite degrees of freedom (DOF) problem into a finite DOF one and then solve it. This paper used Autodesk Inventor to establish the 3D geometry model in **Figure 1**. Ansys was employed in order to analyze the modal and random vibration of the shaft.

High Quality Machinery Steel		
<b>C</b>	0,30-0,38	
<b>Cr</b>	1,30-1,70	
<b>Ni</b>	1,30-1,70	
<b>Mo</b>	0,15-0,30	
<b>Mn</b>	0,70-0,75	
<b>Si</b>	0,09-0,10	
UTS-Rm	Mpa	900-1100
	KSI	130-160
Rp. 0.2%	Mpa	700
	KSI	102
E-A <sub>5</sub>		min.12%
HARDNESS VALUES (BHN)		270-330
EAF + PRE-HARDENED		

**Figure 1** Mechanical properties of HQ705.

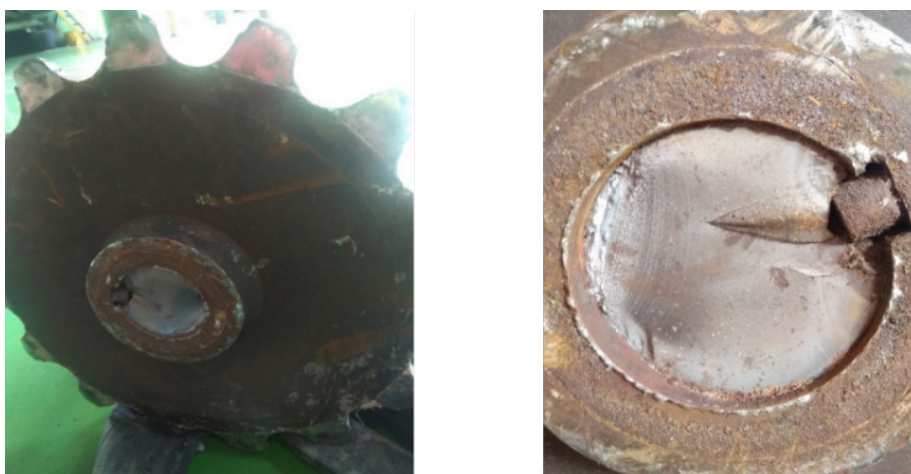


**Figure 2** Photos showing the failure on the shaft sprocket.

First of all, the 3D geometry model of the shaft sprocket was created using Autodesk Inventor. Secondly, the meshing of the 3D geometry meshing model was performed using Ansys, as shown in **Figure 3**. Then, static analysis of the shaft sprocket 3D model was carried out by implementing FEM. The results of static study, such as total deformation, equivalent stress, maximum shear stress and fatigue parameters, will be used for performing modal analysis.

The modal analysis was performed for 6 different modes, and the results were 6 total deformations. Lastly, the random vibration analysis was carried out, and the results were directional deformation, equivalent stress, and shear stress - all of that analysis was performed by implementing FEM in Ansys.

**Figure 3** Meshing of shaft sprocket 3D model.

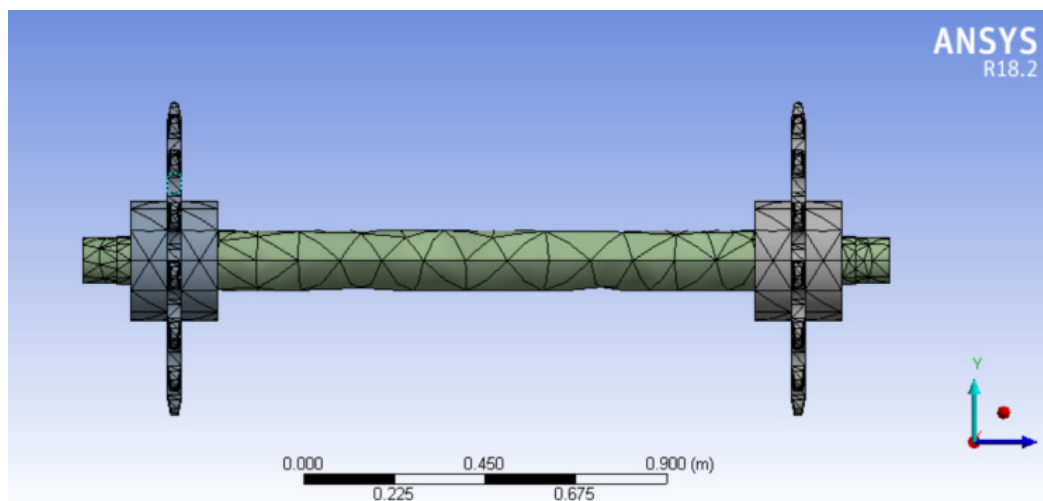


**Table 1** Technical specification of rake conveyor in the Ngadirejo sugar plant.

No.	Station/Equipment name	Type/Merk	Specification
1	Conveyor	Rank conveyor	Bearing sprocket (driver): 22232 CK/C3 Bearing sprocket (driver): 23224 CCK/C3 Bearing rol rake: 6305 2 RSI Number of rol rake: 304 buah Number of rake: 152 buah Rake length: 1545 mm Distance between shaft: 68 m Total deck length: 70 m Deck width: 1660 mm Double deck: 4600 mm Single deck: 2300 mm Number of link: 300 link Number of inner plate: 900 link Number of outner plate: 600 link
2	Conveyor Drive Tranmission	FS 09063 Eaton	Driver chain: Hitachi RS 240 3 strand Driver gear: Z1:20, Z2:27 Driver chain length: 5000 mm Coupling: 1100 T10C

No.	Station/Equipment name	Type/Merk	Specification
3	Driver shaft	-	Diameter: 150 mm Length: 2500 mm Material: HQ 705
4	Driven shaft	-	Diameter: 150 mm Length: 2000 mm Material: HQ 705
5	Gear box	Flender	Power: 100 kW Ratio: 1:38 Rpm: 1485 Driver chain: Rs:240, Z1:20, Z2:50  Bearing: NTN 4T 32312 XL & 32317 U MH Bearing: NTN 30213 & 30230 A Nok seal: TC 150×180×14 & TC 65×85×12
6	Moter driver	MEZ/FRENSTAT/ F 208MU04	Power: 110 kW Rpm: 1485 Input: 380 V Output: 205 A Frequency: 50 HZ

## Results and discussion

### Static analysis

This model uses 8523 nodes and 4118 elements in the mesh. In this analysis, there are 2 fixed supports for the shaft, a load equal to 48000 N on each sprocket, a moment of torque equal to 40000 Nm, and the weight of the shaft, sprockets, and bearing in **Figure 4**. This analysis obtains maximum total deformation equal to 1.1663 mm shown in **Figure 5**, maximum equivalent stress equal to 71.757 MPa, and the minimum life of the shaft is 17.237 cycles, shown in **Figure 6**. The minimum safety factor for this shaft sprocket is 0.55744. The fatigue analysis was carried out using Goodman's criterion.

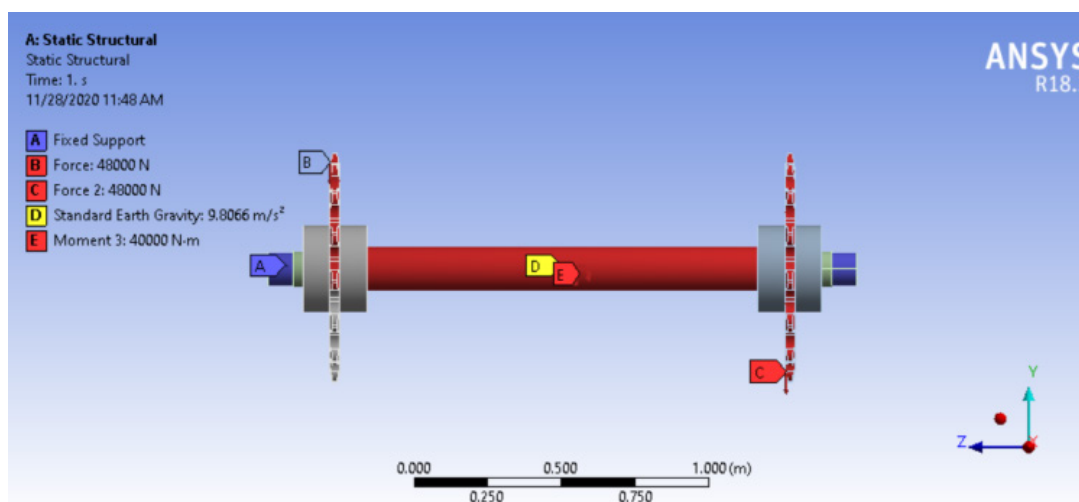


**Figure 4** Load on the shaft sprocket 3D model.

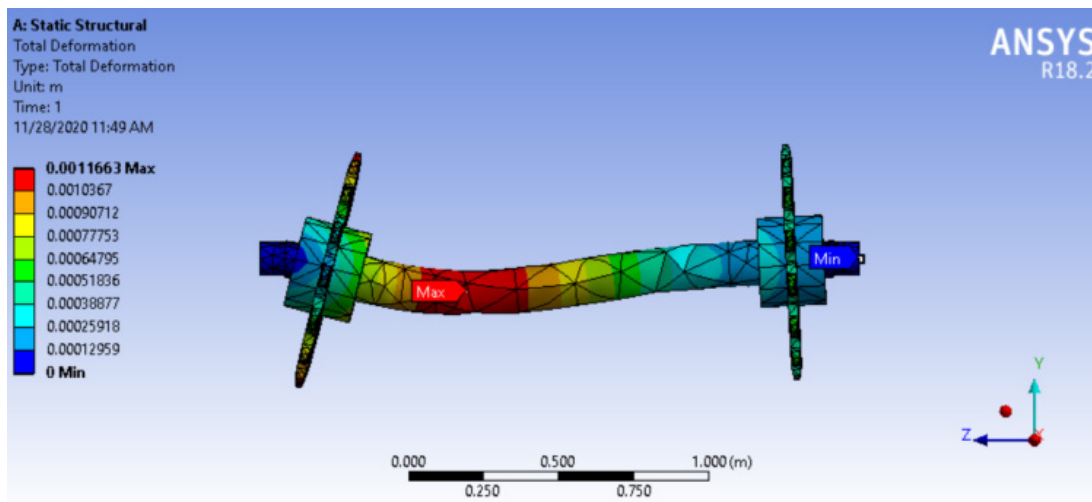


**Figure 5** Total deformation on the shaft sprocket.

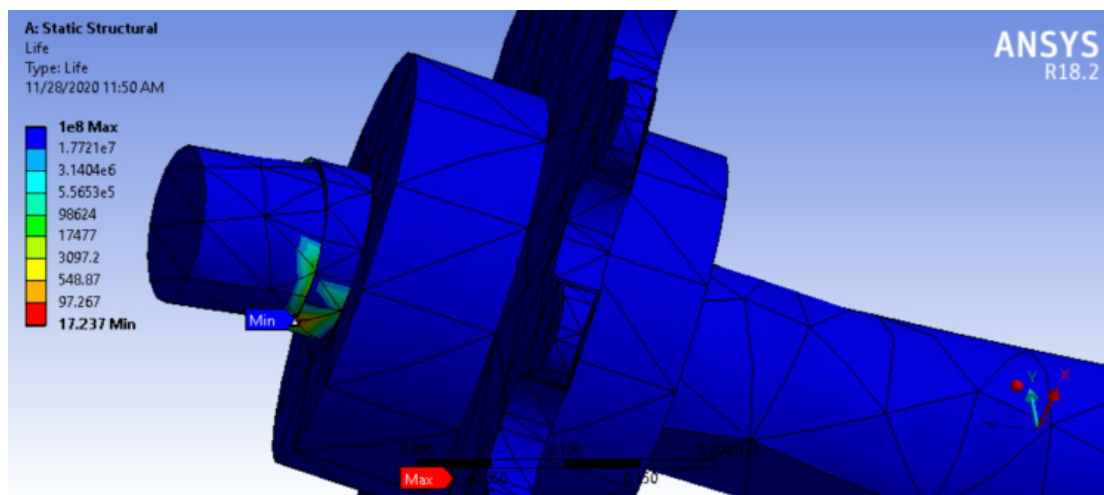


**Figure 6** Life cycle of the shaft sprocket.

### Modal analysis

The results from the analysis shown in **Table 2** conclude that as the order increases, the frequency also increases. The results of modal analysis using Ansys are shown in **Table 2**. Based on the analysis results, the frequency natural in the first mode is 1687.4 Hz, and the maximum deformation is located at the middle of the shaft. In the first mode, the lowest deformation is located in the shaft's fixed point, and the value of its deformation is 0. The deformation value increases from the fixed point toward the middle point of the shaft. The vibration that occurs in the first mode is lateral bending vibration.

The natural frequency in the second mode is 1690.9 Hz, and the maximum deformation is located in the middle of the shaft. In the second mode, the lowest deformation is located at the shaft's fixed point, and the value of its deformation is 0. The deformation value increases from the fixed point toward the middle point of the shaft. The vibration that occurs in the second mode is lateral bending vibration.

**Table 2** Results of modal and frequency analysis .

Mode	Frequency (Hz)
1	1687.4
2	1690.9
3	3061.6
4	3283.1
5	3298.7
6	3384.6

Furthermore, the frequency natural in the third mode is 3061.6 Hz, and the maximum deformation is located at the edge of the sprocket teeth. The minimum deformation is located at the fixed point, and the value is 0. The deformation value increases toward the edge of the sprocket. The vibration that occurs in the third mode is an axial bending vibration. The natural frequency in the fourth mode is 3283.1 Hz. The lowest deformation is located at the fixed point and in the middle of the shaft; the value is 0. The maximum deformation is situated on the edge of the sprocket teeth. The vibration that occurs in the fourth mode is torsional shear vibration.

The fifth mode's natural frequency is 3298.7 Hz. The maximum deformation is located at the edge of sprocket teeth. The minimum deformation is located at the fixed point and in the middle of the shaft. The vibration in this mode is torsional shear vibration. The vibration in this mode is complex compared to the other modes. Lastly, the sixth mode's natural frequency is 3384.6 Hz. The maximum deformation occurs at the edge of the sprocket teeth. The minimum deformation is 0, located at the fixed point and in the middle of the shaft, almost the whole shaft.

The fourth and fifth-order vibrations are very complex from the figures above, especially the latter. These 2 modes include torsional shear vibrations. The first and second-order modes appear to be lateral bending vibration. The third mode is axial bending vibration.

The natural frequency of this shaft changes according to the deformation value, corresponding to Eq. (1) [11].

$$f_n = \frac{1}{2\pi} \sqrt{\frac{989}{\Delta}} \quad (1)$$

The maximum total deformation for the first mode is 2.7495, 2.7516 m for the second mode, 3.2392 m for the third mode, 3.9195 m for the fourth mode, and 3.8048 m for the fifth and 3.292 m for the sixth mode. Thus, we conclude that as the mode's order increases, total deformation also becomes higher. The higher value of displacement means that this design will fail at these specific frequencies, so that these values of frequencies must be avoided in operation.

**Table 3** Maximum stress result.

Mode	Equivalent stress maximum (MPa)	Shear stress maximum (MPa)
1	$1.13 \times 10^5$	$6.20 \times 10^4$
2	$8.91 \times 10^4$	$4.81 \times 10^4$
3	$1.90 \times 10^5$	$1.09 \times 10^5$
4	$1.32 \times 10^5$	$7.12 \times 10^4$
5	$1.80 \times 10^5$	$9.81 \times 10^4$
6	$1.82 \times 10^5$	$1.05 \times 10^6$

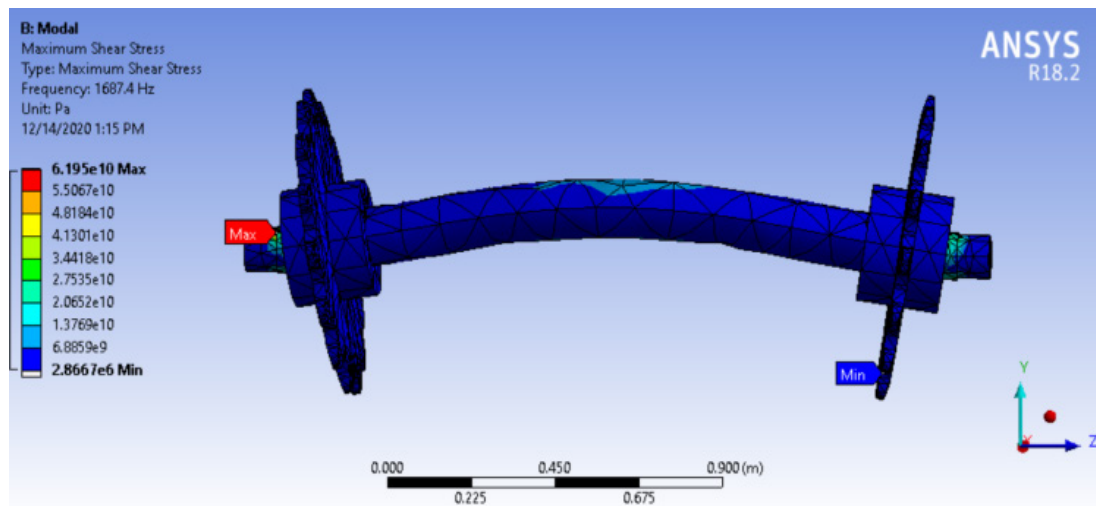


**Figure 7** Maximum shear stress in mode 1.

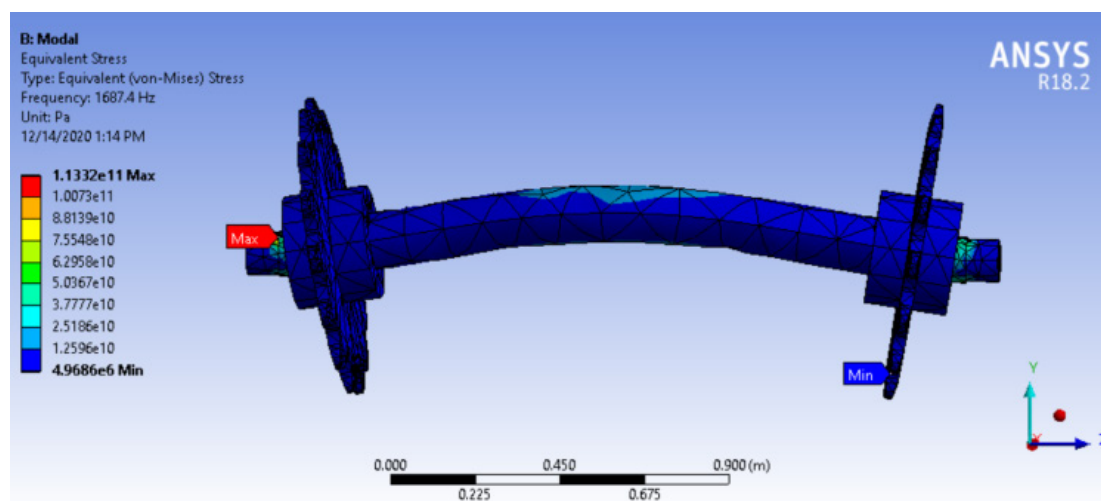


**Figure 8** Maximum equivalent stress in mode 1.

The modal analysis performed in Ansys obtained several data for maximum shear stress, and maximum equivalent stress occurs in the shaft for each mode. The data is shown in **Table 3**. For the first mode, the maximum equivalent stress is  $16.2 \times 10^5$  MPa, and the maximum shear stress is  $1.13 \times 10^4$  MPa. **Figures 7 and 8** show that the maximum shear stress and maximum equivalent stress are located in the same position on the edge between the shaft and the sprocket boss.

Based on the modal analysis, the maximum shear stress and maximum equivalent stress are located in the same position. The maximum equivalent stress and maximum shear stress values are  $8.91 \times 10^4$  MPa and  $4.81 \times 10^4$  MPa, respectively. The analysis shows that the maximum shear stress for the third mode is  $1.0942 \times 10^5$  MPa and the maximum equivalent stress is  $1.895 \times 10^5$  MPa. As we can see in **Figure 20 and 21**, maximum shear stress and maximum equivalent stress occur in the exact location, which is at the edge between the shaft and sprocket boss.

Based on the modal analysis, the maximum shear stress and maximum equivalent stress are located in the same position. The maximum equivalent stress and maximum shear stress values are  $1.32 \times 10^5$  and  $7.12 \times 10^4$  MPa, respectively.

Based on the modal analysis, the maximum equivalent stress is  $1.80 \times 10^5$  MPa, and the maximum shear stress is  $9.81 \times 10^4$  MPa for the fifth mode. Both maximum stresses occur in the exact location. Lastly, for the sixth mode, the maximum shear stress is  $1.05 \times 10^5$  MPa, and the maximum equivalent stress is  $1.82 \times 10^5$  MPa. In this mode, the maximum shear and equivalent stress also occur in the same location. The location where maximum shear and equivalent stress of the first, second, third, fifth, and

sixth appear is the critical part of the shaft sprocket. In reality, the failure of the shaft sprocket occurs in this exact location. Thus, it is essential to pay attention to this very location.

**Table 4** Participation factor of modes analysis.

Mode	Freq (Hz)	X direction	Y direction	Z direction	Rotation X	Rotation Y	Rotation Z
1	1687.4	-0.24484	0.48044	$7.08 \times 10^{-5}$	$-1.41 \times 10^{-3}$	$-7.02 \times 10^{-4}$	-0.14309
2	1690.9	0.48042	0.24454	$3.89 \times 10^{-4}$	$-5.16 \times 10^{-5}$	$5.70 \times 10^{-4}$	-0.19919
3	3061.6	$9.10 \times 10^{-4}$	$2.42 \times 10^{-4}$	$-8.20 \times 10^{-5}$	$-5.94 \times 10^{-4}$	$-2.60 \times 10^{-3}$	0.1243
4	3283.1	$5.09 \times 10^{-4}$	$-1.14 \times 10^{-3}$	$4.84 \times 10^{-3}$	-0.21125	0.11842	$7.23 \times 10^{-4}$
5	3298.7	$-5.97 \times 10^{-4}$	$-4.78 \times 10^{-4}$	$4.88 \times 10^{-3}$	-0.11471	-0.21125	$-6.75 \times 10^{-4}$
6	3384.6	$4.60 \times 10^{-4}$	$2.67 \times 10^{-4}$	$1.11 \times 10^{-4}$	$2.09 \times 10^{-4}$	$-6.71 \times 10^{-3}$	$-3.17 \times 10^{-3}$

As discussed in the previous paragraph, there are 6 modes generated from the modal analysis by using Ansys. The modal analysis results vary, and not all of them are necessarily considered to have a conclusion. In order to understand the most critical parameters, there must be a participation factor of mode analysis data. **Table 4** shows the result of the participation factor from the analysis of the modes, as shown in **Table 4**. The most participated parameter has the highest value in that table, which is 0.48044 in the Y direction for the first mode, and the frequency is 1687.4 Hz, so that the only mode that needs to be considered is the first mode in the Y direction because the value of its participation factor is the highest.

#### Random vibration analysis

Based on the random vibration analysis in **Figure 29** and **30**, the maximum equivalent stress is 7314.7 GPa, and the maximum shear stress on the YZ plane is 2573.1 GPa. The random vibration analysis on a scale factor value of 1 sigma with a probability of 68.269 %.

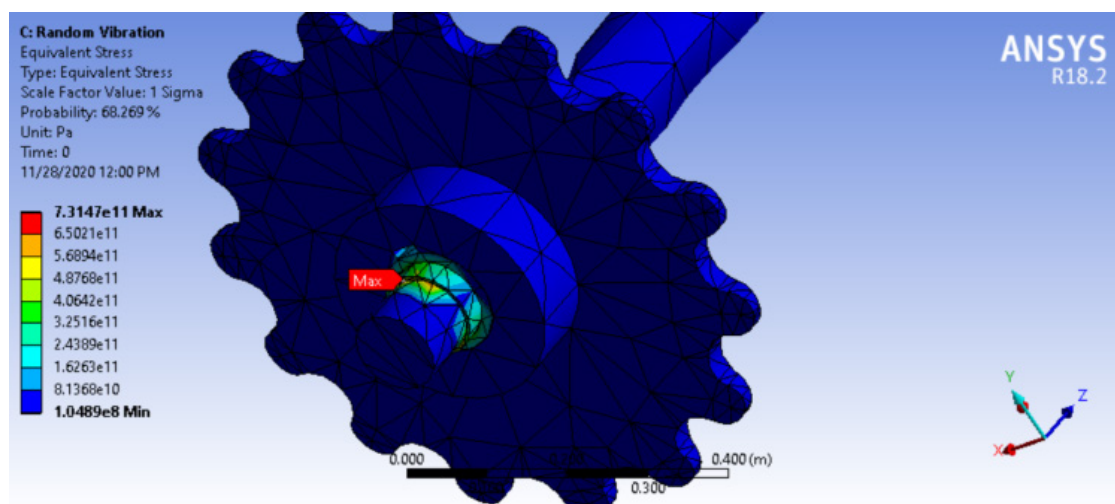


**Figure 9** Equivalent stress of the shaft sprocket for random vibration.

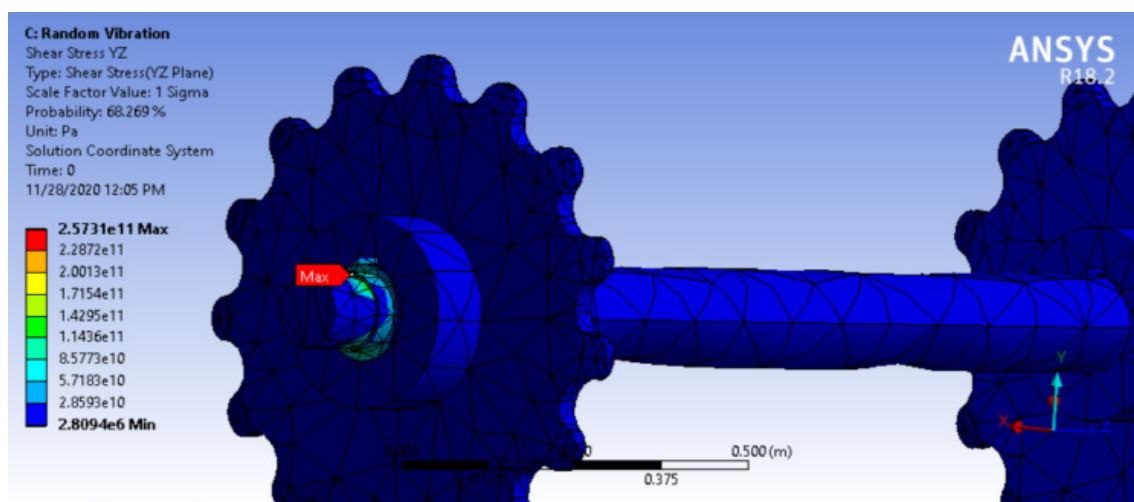


**Figure 10** Shear stress of the shaft sprocket for random vibration.

## Conclusions

Static, modal, and random vibration analyses were performed in this study. The maximum deformation, as determined by static analysis, is 1.1663 mm, whereas the maximum life cycle is  $1 \times 10^8$ . When performing modal analysis, as the order number increases, the frequency and maximum deformation increase proportionately. The vibration of the fourth and fifth orders contains the most sophisticated form of torsional shear vibration. According to participation factor statistics, the initial mode in the Y direction has the greatest value of 0.48044. Maximum equivalent stress and maximum shear stress occur precisely at the point of analysis for static, modal, and random vibrations. That analysis is pertinent to the real-world failure that occurred.

## Acknowledgments

The author would like to thank the University of 17 Agustus 1945 Surabaya. This work will not be done without financial and mental support from the institution.

## References

- [1] AH Ertas, V Alkan and AF Yilmaz. Finite element simulation of a mercantile vessel shipboard under working conditions. *Proc. Eng.* 2014; **69**, 1001-7.
- [2] X Zexiao, W Jianguo and Z Qiumei. Complete 3D measurement in reverse engineering using a multiprobe system. *Int. J. Mach. Tool. Manufact.* 2005; **45**, 1474-86.
- [3] SK Singh, V Kumar, PP Reddy and AK Gupta. Finite element simulation of ironing process under warm conditions. *J. Mater. Res. Tech.* 2014; **3**, 71-8.
- [4] EA Al-Bahkali and AT Abbas. Failure analysis of vise jaw holders for hacksaw machine. *J. King Saud Univ. Eng. Sci.* 2016; **30**, 68-77
- [5] R Bardell, V Balendran and K Sivayoganathan. Accuracy analysis of 3D data collection and free-form modeling methods. *J. Mater. Process. Tech.* 2003; **133**, 26-33.
- [6] SM Hussaini, SK Singh, AK Gupta. Experimental and numerical investigation of formability for austenitic stainless steel 316 at elevated temperatures. *J. Mater. Res. Tech.* 2014; **3**, 17-24.
- [7] AH Ertas and FO Sonmez. A parametric study on fatigue strength of spot-weld joints. *Fatig. Fract. Eng. Mater. Struct.* 2008; **31**, 766-76
- [8] SO Afolabi, BI Oladapo, CO Ijagbemi, AOM Adeoye and JF Kayode. Design and finite element analysis of fatigue life prediction for safe and economical machine shaft. *J. Mater. Res. Tech.* 2019; **8**, 105-11.
- [9] B Minghwa, R Subo and Z Haiwu. FEM analysis and design of sprocket connecting shaft in sintering machine. In: Proceedings of the WASE International Conference of Information Engineering, Washington DC, United States. 2010, p. 144-7.

- 
- [10] B Bai, L Zhang, T Guo and C Liu . Analysis of dynamic characteristics of the main shaft system in a hydro-turbine based on ANSYS. *Proc. Eng.* 2012; **31**, 654-8.
- [11] L Frizziero and L Piancastelli. Accelerated FEM analysis for critical engine components. *Walailak J. Sci. & Tech.* 2014; **12**, 151-65.
- [12] GV Zyl and A Al-Sahli. Failure analysis of conveyor pulley shaft. *Case Stud. Fail. Anal.* 2013; **1**, 144-55.
- [13] RS Khurmi and JK Gupta. *A text book of machine design*. Eurasia Publishing House (PVT.), New Delhi, 2005.
- [14] MTA Ofrial, L Noerochim and MIP Hidayat. Analisis numerikal frekuensi natural pada poros low pressure boiler feed pump PT.PJB UP Gresik. *Jurnal Teknik ITS* 2017; **6**, F1-F6.
- [15] PT Tira Austenite Tbk. *HQ Series: Machinery Steel Series*. PT Tira Austenite Tbk, Indonesia, 2020.
- [16] YMM Reddy and PR Chander. Fatigue analysis of chain sprocket using finite element analysis. *Int. J. Adv. Eng. Res. Dev.* 2018; **5**, 917-22.
- [17] R Suthar. Analysis of sprocket strength finite element analysis method. *Int. J. Adv. Manag. Tech. Eng. Sci.* 2017; **7**, 109-19.
- [18] K Satishkumar and N Ugesh. Finite element analysis of a shaft subjected to a load. *ARPN J. Eng. Appl. Sci.* 2006; **11**, 5996-6000.